

## INFLUENCE OF THE SPECTRAL IMAGE COMPONENT ON THE AMPLITUDE AND PHASE ESTIMATORS PROVIDED BY THE INTERPOLATED DFT METHOD

Daniel BELEGA<sup>1</sup>, Dario PETRI<sup>2</sup>, Dominique DALLET<sup>3</sup>

<sup>1</sup>“Politehnica” University of Timișoara, Department of Measurements and Optical Electronics,  
Bv. V. Pârvan, Nr. 2, 300223, Timișoara, Romania,

E-mail: daniel.belega@upt.ro

<sup>2</sup> University of Trento, Department of Industrial Engineering,  
Trento 38123, Italy,

E-mail: dario.petri@unitn.it

<sup>3</sup> University of Bordeaux, IMS Laboratory, Bordeaux INP,  
CNRS UMR5218, France,

E-mail: dominique.dallet@ims-bordeaux.fr

Corresponding author: Daniel BELEGA, E-mail: daniel.belega@upt.ro

**Abstract.** In this paper the contribution of the spectral image of a sine-wave fundamental component on the amplitude and phase estimators provided by the Interpolated Discrete Fourier Transform (IpDFT) method based on the Maximum Sidelobe Decay (MSD) windows is analyzed. In particular, accurate analytical expressions for the amplitude and phase estimation errors are proposed. Leveraging on these expressions, amplitude and phase estimators that compensate the above detrimental contribution are proposed. The accuracies of the derived expressions are verified through computer simulations. Simulations are then used also to compare the accuracies of the uncompensated and compensated amplitude and phase estimators.

**Key words:** error analysis, interpolated DFT method, parameter estimation, sine-wave, windowing.

### 1. INTRODUCTION

In many engineering applications such as audio, radar, instrumentation, power systems, and vibration analysis, sine-waves are employed and their parameters need to be accurately estimated in real-time. For this purpose frequency domain based procedures are commonly employed. One widely adopted frequency domain procedure is the so-called Interpolated Discrete Fourier Transform (IpDFT) method [1–11]. Firstly it compensates the contribution of picket-fence effect on the estimated sine-wave parameters by determining the inter-bin frequency location of the acquired sine-wave. This task is performed by interpolating the two highest DFT spectral samples. Then, the sine-wave amplitude and phase are estimated using the derived inter-bin frequency location value. To reduce the contribution on the estimated parameters due to spectral leakage from the image component and other disturbances such as harmonics and inter-harmonics, the analyzed signal is usually weighted by a suitable window function. Windows belonging to the cosine-class [12, 13] are usually employed. In particular, when the Maximum Sidelobe Decay (MSD) windows are adopted the sine-wave parameter estimators returned by the IpDFT method are given by simple and accurate analytical expressions [1, 3–5]. Moreover, these windows ensure a high spectral leakage rejection since the  $H$ -term MSD window ( $H \geq 2$ ) has the highest sidelobe decay rate, equal to  $6(2H - 1)$  dB/octave, among all the  $H$ -term cosine windows.

The IpDFT method estimates the inter-bin frequency location by assuming that the contribution of the spectral image of the fundamental component is negligible. Therefore, the returned estimates are biased by that contribution, which can be relevant when a small number of sine-wave cycles is observed. In [6] an analytical expression for the related frequency estimation error has been derived. However, expressions for the contribution of the spectral image of the fundamental component on the estimated sine-wave amplitude

and phase have not been derived yet in the scientific literature. These expressions are very useful in practice since they allow the compensation of the above detrimental contribution on the amplitude and phase estimation. Hence, the goal of this paper is to derive the above expressions when an MSD window is used.

The remaining of the paper is organized as follows. In Section 2 the sine-wave parameter estimators provided by the IpDFT method based on an  $H$ -term MSD ( $H \geq 2$ ) windows are shortly presented. In Section 3 the expressions for the amplitude and the phase errors due to the effect of the spectral image of the fundamental component are derived and their behaviors are analyzed. Moreover, leveraging on the derived expressions, amplitude and phase estimators that compensate the contribution of the interference from the spectral image of the fundamental component are proposed. The accuracies of the derived expressions and the main properties of amplitude and phase errors are verified through computer simulations in Section 4. Also, the accuracies of the compensated estimators are compared with those provided by the classical IpDFT method by using simulations. Finally, Section 5 concludes this work.

## 2. THEORETICAL BACKGROUND

The analyzed discrete-time sine-wave is modeled as:

$$x(m) = A \sin(2\pi f m + \phi), \quad m = 0, 1, 2, \dots, M - 1 \quad (1)$$

where  $A$ ,  $f$ , and  $\phi$  are the amplitude, normalized frequency, and initial phase parameters, and  $M$  is the number of analyzed samples. The normalized frequency  $f$  is expressed by:

$$f = \frac{f_{in}}{f_s} = \frac{\nu}{M} = \frac{l + \delta}{M}, \quad (2)$$

where  $f_{in}$  is the frequency of the continuous-time sine-wave,  $f_s$  is the sampling frequency,  $\nu = l + \delta$  is the number of acquired sine-wave cycles or the normalized frequency expressed in bins, where  $l$  is the integer part of  $\nu$  and  $\delta$  ( $-0.5 \leq \delta < 0.5$ ) is the inter-bin frequency location. In the following it is assumed  $f < 0.5$  to satisfy the Nyquist theorem.

In most encountered practical situations the sampling process is non-coherent, i.e.  $\delta \neq 0$ , so that spectral leakage and picket-fence effects occur [14]. To reduce spectral leakage windowing is applied to the analyzed signal, while picket-fence effect is compensated by IpDFT method.

In the following the  $H$ -term MSD window ( $H \geq 2$ ) is considered. It is defined as:

$$w(m) = \sum_{h=0}^{H-1} (-1)^h a_h \cos\left(2\pi h \frac{m}{M}\right), \quad m = 0, 1, \dots, M - 1 \quad (3)$$

in which  $a_h$ ,  $h = 0, 1, \dots, H - 1$  are the window coefficients, with [5]:  $a_0 = C_{2H-2}^{H-1} / 2^{2H-2}$ ,  $a_h = C_{2H-2}^{H-h-1} / 2^{2H-3}$ ,  $h = 1, 2, \dots, H - 1$ , where  $C_m^p = m! / ((m-p)! p!)$ ,

The Discrete-Time Fourier Transform (DTFT) of the windowed signal  $x_w(m) = x(m) \cdot w(m)$ ,  $m = 0, 1, \dots, M - 1$ , is given by:

$$X_w(\lambda) = \frac{A}{2j} [W(\lambda - \nu) e^{j\phi} - W(\lambda + \nu) e^{-j\phi}] \quad (4)$$

where  $W(\cdot)$  represents the DTFT of the window  $w(\cdot)$ . When  $M$  is high, as occurs in many engineering applications, and  $|\lambda| \ll M$ , with high accuracy we have [5]:

$$W(\lambda) = \frac{M \sin(\pi\lambda)}{2^{2H-2} \pi\lambda} \frac{(2H-2)!}{\prod_{h=1}^{H-1} (h^2 - \lambda^2)} e^{-j\pi\lambda}, \quad \text{for } |\lambda| \ll M. \quad (5)$$

It is worth noticing that the second term in (4) represents the spectral image of the fundamental component. Assuming that the related contribution to the DFT samples  $X_w(l+i)$ ,  $i = 0, \pm 1$  is negligible, the inter-bin

frequency location estimator provided by the IpDFT method based on the  $H$ -term MSD window ( $H \geq 2$ ) is given by [1, 5]:

$$\hat{\delta} = \frac{(H+i-1)\alpha - H+i}{\alpha+1}, \quad (6)$$

where  $\alpha = |X_w(l+i)|/|X_w(l-1+i)|$ , in which  $i=0$  if  $|X_w(l-1)| \geq |X_w(l+1)|$  and  $i=1$  if  $|X_w(l-1)| < |X_w(l+1)|$ .

Moreover, the related amplitude and phase estimators are [4]:

$$\hat{A} = 2 \frac{|X_w(l)|}{|W(-\hat{\delta})|}, \quad (7)$$

and

$$\hat{\phi} = \text{angle}\{X_w(l)\} - \pi\hat{\delta} + \frac{\pi}{2}, \quad (8)$$

where  $\hat{\delta}$  is given by (6).

### 3. THE EXPRESSIONS FOR THE AMPLITUDE AND PHASE ESTIMATION ERRORS DUE TO THE SPECTRAL IMAGE COMPONENT

An accurate analytical expression for the amplitude relative estimation error due to the spectral image component is given in the following proposition (see the proof in Appendix A).

**PROPOSITION 1.** *When using the IpDFT method based on the  $H$ -term MSD window ( $H \geq 2$ ), the amplitude relative estimation error due to the spectral image of the sine-wave fundamental component is given by:*

$$\begin{aligned} \varepsilon_A &= \frac{\Delta A}{A} = \frac{\hat{A} - A}{A} \cong -\frac{\tilde{W}'(\delta)}{\tilde{W}(\delta)} \Delta\delta + p \frac{\tilde{W}(2l+\delta)}{\tilde{W}(\delta)} \cos(2\pi\delta + 2\phi) \\ &\cong p \left[ (-1)^{i+1} \frac{2(l+\delta)(H-|\delta|)}{2l+\delta+(-1)^{i+1}H} \frac{\tilde{W}'(\delta)}{\tilde{W}(\delta)} + 1 \right] \frac{\tilde{W}(2l+\delta)}{\tilde{W}(\delta)} \cos(2\pi\delta + 2\phi), \end{aligned} \quad (9)$$

where  $\tilde{W}(\lambda) = |W(\lambda)|$ ,  $\tilde{W}'(\lambda)$  is the derivative of  $\tilde{W}(\lambda)$  with respect to  $\lambda$ ,  $\Delta\delta$  is the inter-bin frequency location estimation error due to the spectral image component (see (A.8) in Appendix A), and  $p = (-1)^H \text{sgn}(\delta)$ , in which  $\text{sgn}(\cdot)$  is the sign function.

It is worth noticing that  $\tilde{W}(\cdot)$  is an even function, while  $\tilde{W}'(\cdot)$  is an odd function with  $\tilde{W}'(\delta) > 0$  when  $-0.5 < \delta < 0$  and  $\tilde{W}'(\delta) < 0$  when  $0 < \delta < 0.5$ .

An accurate analytical expression for the phase estimation error due to the spectral image component is given in the following proposition (see the proof in Appendix B).

**PROPOSITION 2.** *When using the IpDFT method based on the  $H$ -term MSD window ( $H \geq 2$ ), the phase estimation error due to the spectral image of the sine-wave fundamental component is given by:*

$$\begin{aligned} \Delta\phi = \hat{\phi} - \phi &\cong -\pi\Delta\delta + p \frac{\tilde{W}(2l+\delta)}{\tilde{W}(\delta)} \cos\left(2\pi\delta + 2\phi + \frac{\pi}{2}\right) = \\ &\cong p \left[ (-1)^{i+1} \frac{2\pi(l+\delta)(H-|\delta|)}{2l+\delta+(-1)^{i+1}H} \cos(2\pi\delta + 2\phi) + \cos\left(2\pi\delta + 2\phi + \frac{\pi}{2}\right) \right] \frac{\tilde{W}(2l+\delta)}{\tilde{W}(\delta)}. \end{aligned} \quad (10)$$

From expressions (9) and (10) the following remarks can be drawn:

- $\varepsilon_A$  has two errors components which behave like a cosine function; only the first component depends on the frequency error  $\Delta\delta$ ;
- due to the sign of  $\tilde{W}'(\delta)$  and the value of  $i$  the error components of  $\varepsilon_A$  provide opposite contributions, thus partially compensating each other;
- $\Delta\phi$  has two errors components which behave like cosine functions, whose arguments differ by  $\pi/2$  rad; only the first component depends on the frequency error  $\Delta\delta$ , while the second component is smaller than the first one since  $H \geq 2$  and assuming  $l \geq 2$  cycles;
- when coherent sampling occurs, since  $\tilde{W}(2l) = 0$  for  $l > H/2$  cycles both  $\varepsilon_A$  and  $\Delta\phi$  are nulls;
- when  $\nu > H/2$ , both  $\varepsilon_A$  and  $\Delta\phi$  decreases as  $H$  increases.

Expressions (9) and (10) allow us to propose the following amplitude and phase estimators which compensate the contribution of the spectral image of the fundamental component:

$$\hat{A}_c = \hat{A} \left\{ 1 - p \left[ (-1)^{i+1} \frac{2(l + \hat{\delta})(H - |\hat{\delta}|)}{2l + \hat{\delta} + (-1)^{i+1}H} \frac{\tilde{W}'(\hat{\delta})}{\tilde{W}(\hat{\delta})} + 1 \right] \frac{\tilde{W}(2l + \hat{\delta})}{\tilde{W}(\hat{\delta})} \cos(2\pi\hat{\delta} + 2\hat{\phi}) \right\}, \quad (11)$$

and

$$\hat{\phi}_c = \hat{\phi} - p \left[ (-1)^{i+1} \frac{2\pi(l + \hat{\delta})(H - |\hat{\delta}|)}{2l + \hat{\delta} + (-1)^{i+1}H} \cos(2\pi\hat{\delta} + 2\hat{\phi}) + \cos\left(2\pi\hat{\delta} + 2\hat{\phi} + \frac{\pi}{2}\right) \right] \frac{\tilde{W}(2l + \hat{\delta})}{\tilde{W}(\hat{\delta})}, \quad (12)$$

where  $\hat{\delta}$ ,  $\hat{A}$ , and  $\hat{\phi}$  are the estimators for the parameters  $\delta$ ,  $A$ , and  $\phi$ , respectively, provided by the IpDFT method.

It is worth noticing that when  $\nu$  is high enough the contribution of the spectral image of the fundamental component becomes negligible. As a consequence the compensated estimators are almost equal to those provided by the IpDFT method.

#### 4. COMPUTER SIMULATIONS

In this Section, computer simulations are employed, at first, to verify the accuracies of expressions (9) and (10) for the amplitude relative estimation error  $\varepsilon_A$  and the phase estimation error  $\Delta\phi$ . Then, simulations will allow to compare the accuracies of the compensated amplitude and phase estimators (11) and (12) and the classical the IpDFT method.

Simulation results reported in the following are obtained considering the amplitude of the simulated sine-waves  $A = 1$ , the number of analyzed samples  $M = 512$  and the two-term MSD window (also known as Hann window) or the three-term MSD windows[13].

Figure 1 shows both the theoretical and the simulation results for the amplitude relative estimation error  $\varepsilon_A$  (Fig. 1a) and phase error  $\Delta\phi$  (Fig. 1b) as a function of the sine-wave phase  $\phi$  for  $\nu = 2.75$  and  $3.25$  bins when the two- or three-term MSD windows are adopted. The phase  $\phi$  was varied in the range  $[0, 360]$  deg. with a step of  $3.6$  deg.

In Figure 1 it can be observed that the simulation and theoretical results are in very good agreement. Moreover, it can be seen that both errors  $\varepsilon_A$  and  $\Delta\phi$  decreases as  $H$  increases, as expected from the theoretical expressions (9) and (10), respectively.

It is worth noticing that many other simulations were performed using different values for the parameters. However, behaviors very similar to those reported in Fig. 1 have been always obtained for the amplitude estimation error, the phase estimation error and their respective components as soon as  $\nu > 1.5$  bins.

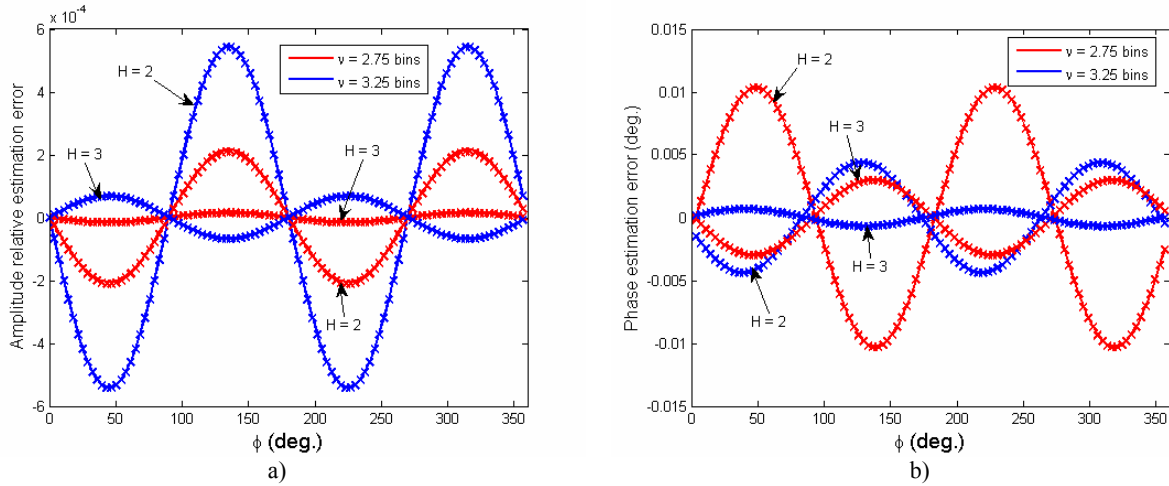


Fig. 1 – Amplitude relative estimation error  $\varepsilon_A$  (a) and phase estimation error  $\Delta\phi$  (b) *versus* sine-wave phase  $\phi$  when  $\nu = 2.75$  and  $3.25$  cycles are observed and  $M = 512$  samples are analyzed. Two-term or three-term (b) MSD windows. The results returned by (9) and (10) are marked by crosses ('x').

To model real-life situations, the accuracies of the uncompensated and the compensated estimators are compared in the case of sine-waves corrupted by additive white Gaussian noise. The Mean Square Error (MSE) is used as accuracy parameter since it includes both the bias due to the interference from the spectral image of the fundamental component and the variance due to wideband noise. Figure 2 shows the MSEs of the estimators  $\hat{A}$  and  $\hat{A}_c$  (Fig. 2a) and of the estimators  $\hat{\phi}$  and  $\hat{\phi}_c$  (Fig. 2b) as a function of the number of observed sine-wave cycles  $\nu$  in the case of noisy sine-waves characterized by Signal-to-Noise Ratio (SNR) equal to 40 dB. The number of observed cycles  $\nu$  has been varied in the range [1.51, 8) bins with a step of 0.05 bins. For each value of  $\nu$ , 1 000 records of  $M = 512$  sample each have been generated by choosing the sine-wave phase  $\phi$  at random in the range  $[0, 2\pi)$ . The Hann window has been adopted.

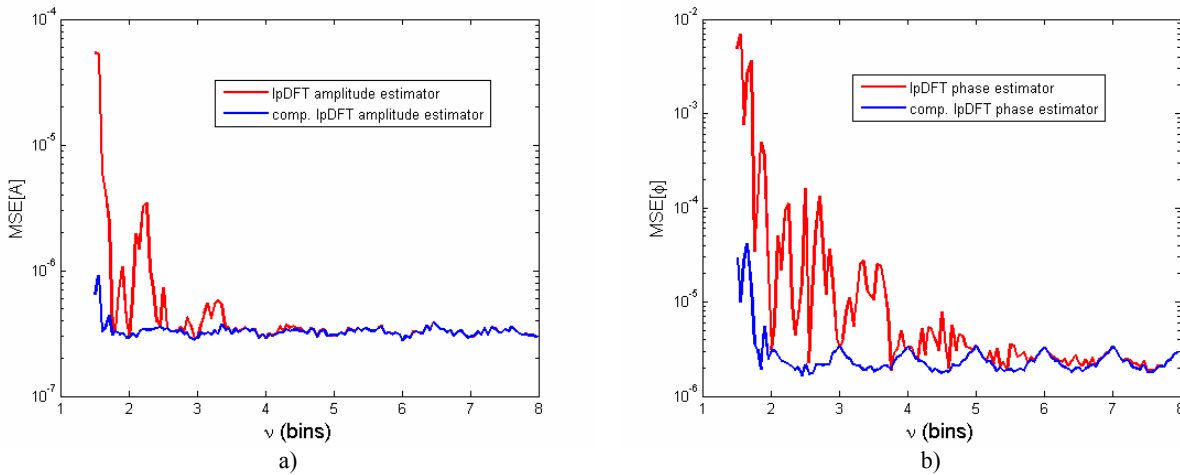


Fig. 2 – MSEs of the estimators  $\hat{A}$  and  $\hat{A}_c$  (a) and of the estimators  $\hat{\phi}$  and  $\hat{\phi}_c$  (b) *versus* the sine-wave cycles  $\nu$  in the case of noisy sine-waves with SNR = 40 dB. The estimators  $\hat{A}$  and  $\hat{\phi}$  are provided by the classical IpDFT method, while the estimators  $\hat{A}_c$  and  $\hat{\phi}_c$  are expressed by (11) and (12), respectively. Two-term MSD window and 1 000 runs of  $M = 512$  samples are considered.

Figure 2 shows that the compensated estimators  $\hat{A}_c$  and  $\hat{\phi}_c$  are more accurate than the estimators  $\hat{A}$  and  $\hat{\phi}$  provided by the classical IpDFT method when the interference from the spectral image of the fundamental component prevails over wideband noise, that is for small values of the number of observed cycles  $\nu$ . The

value of  $\nu$  up to which that behavior occurs increases as SNR increases. For high values of  $\nu$  wideband noise becomes dominant and the accuracies of both compensated and uncompensated estimators are almost equal as expected from theory. For very small values of  $\nu$  the compensated estimators exhibit low accuracy since the IpDFT estimators adopted for the image effect compensation are very poor. Quite interestingly, by comparing the results in Figs. 2a) and b) it follows that the phase estimator is more sensitive to the interference from the spectral image of the fundamental component than the amplitude estimator.

## 5. CONCLUSIONS

This paper has been aimed at the derivation of the amplitude and phase estimation errors due to the spectral image of a sine-wave fundamental component when the IpDFT method based on the MSD windows is employed. In practice these errors often prevail over other estimation uncertainty contributions such as spurious tones or wideband noise when few sine-wave cycles are observed. It has been shown that both amplitude and phase errors exhibit two different components. The first one depends on the frequency estimation error, while the other one heavily depends on the number of observed sine-wave cycles. In particular, while the components of the amplitude estimation error have opposite signs, thus compensating their effects, the phase error mainly depends only on the frequency estimation error. In addition, both amplitude and phase errors exhibit a cosine behavior with respect to the sine-wave phase. Leveraging on the derived expressions, amplitude and phase estimators that compensate the spectral image contribution have been proposed. Computer simulations showed that the compensated estimators outperform those provided by the IpDFT method when few sine-wave cycles are observed.

## APPENDIX A

### EXPRESSION FOR THE AMPLITUDE RELATIVE ESTIMATION ERROR

The DFT spectral sample  $|X_w(l)|$  is given by [15]:

$$|X_w(l)| \cong \frac{A}{2} [\tilde{W}(\delta) + p\tilde{W}(2l + \delta)\cos(2\pi\delta + 2\phi)], \quad (\text{A.1})$$

where  $p = (-1)^H \text{sgn}(\delta)$ , in which  $\text{sgn}(\cdot)$  is the sign function, and  $\tilde{W}(\lambda) = |W(\lambda)|$ . By replacing (A.1) in (7) it follows that:

$$\hat{A} \cong \frac{A[\tilde{W}(\delta) + p\tilde{W}(2l + \delta)\cos(2\pi\delta + 2\phi)]}{\tilde{W}(\hat{\delta})}. \quad (\text{A.2})$$

Since the error  $\Delta\delta = \hat{\delta} - \delta$  is very small,  $\tilde{W}(\hat{\delta})$  can be well approximated by using the Taylor's series about  $\delta$  truncated to the first order term:

$$\tilde{W}(\hat{\delta}) \cong \tilde{W}(\delta) + \tilde{W}'(\delta)\Delta\delta, \quad (\text{A.3})$$

where  $\tilde{W}'(\delta)$  is the derivative of  $\tilde{W}(\cdot)$  with respect to  $\delta$ . By substituting (A.3) into (A.2) we obtain:

$$\hat{A} \cong A \frac{1 + p \frac{\tilde{W}(2l + \delta)}{\tilde{W}(\delta)} \cos(2\pi\delta + 2\phi)}{1 + \frac{\tilde{W}'(\delta)}{\tilde{W}(\delta)} \Delta\delta}. \quad (\text{A.4})$$

Since  $\tilde{W}(\delta) \gg \tilde{W}'(\delta)\Delta\delta$ , using the approximation  $(1+x)^{-1} \cong 1-x$ , when  $|x| \ll 1$ , and neglecting the term containing the product  $\tilde{W}(2l+\delta) \cdot \tilde{W}'(\delta)$  because it is negligible as compared with the other terms, after simple algebra we obtain:

$$\hat{A} \cong A \left[ 1 - \frac{\tilde{W}'(\delta)}{\tilde{W}(\delta)} \Delta\delta + p \frac{\tilde{W}(2l+\delta)}{\tilde{W}(\delta)} \cos(2\pi\delta + 2\phi) \right]. \quad (\text{A.5})$$

From (A.5) it follows that the amplitude relative estimation error is given by:

$$\varepsilon_A \stackrel{\Delta}{=} \frac{\Delta A}{A} \cong - \frac{\tilde{W}'(\delta)}{\tilde{W}(\delta)} \Delta\delta + p \frac{\tilde{W}(2l+\delta)}{\tilde{W}(\delta)} \cos(2\pi\delta + 2\phi). \quad (\text{A.6})$$

Since the error  $\Delta\delta$  due to the spectral image component is given by [6]:

$$\Delta\delta \cong (-1)^i p \frac{2(l+\delta)(H-|\delta|)}{2l+\delta+(-1)^{i+1}H} \frac{\tilde{W}(2l+\delta)}{\tilde{W}(\delta)} \cos(2\pi\delta + 2\phi). \quad (\text{A.7})$$

replacing (A.7) into (A.6), expression (9) is finally achieved.

## APPENDIX B

### EXPRESSION FOR THE PHASE ESTIMATION ERROR

From (4) and (5) it follows that:

$$X_w(l) = \frac{A}{2j} \left[ \tilde{W}(\delta) e^{j(\pi\delta+\phi)} + p \tilde{W}(2l+\delta) e^{-j(\pi\delta+\phi)} \right]. \quad (\text{B.1})$$

from which:

$$\text{angle}\{X_w(l)\} = -\frac{\pi}{2} + \tan^{-1} \left\{ \frac{\tilde{W}(\delta) - p\tilde{W}(2l+\delta)}{\tilde{W}(\delta) + p\tilde{W}(2l+\delta)} \tan(\pi\delta + \phi) \right\}, \quad (\text{B.2})$$

where  $\tan^{-1}(\cdot)$  is the arctangent function.

Since  $\tilde{W}(\delta) \gg \tilde{W}(2l+\delta)$ , using the approximation  $(1+x)^{-1} \cong 1-x$ , when  $|x| \ll 1$ , we obtain:

$$\tan^{-1} \left\{ \frac{\tilde{W}(\delta) - p\tilde{W}(2l+\delta)}{\tilde{W}(\delta) + p\tilde{W}(2l+\delta)} \tan(\pi\delta + \phi) \right\} \cong \tan^{-1} \left\{ \left[ 1 - p \frac{\tilde{W}(2l+\delta)}{\tilde{W}(\delta)} \right]^2 \tan(\pi\delta + \phi) \right\}. \quad (\text{B.3})$$

Since the square of the ratio  $\tilde{W}(2l+\delta) / \tilde{W}(\delta)$  is negligible as compared to the other terms it follows that:

$$\tan^{-1} \left\{ \frac{\tilde{W}(\delta) - p\tilde{W}(2l+\delta)}{\tilde{W}(\delta) + p\tilde{W}(2l+\delta)} \tan(\pi\delta + \phi) \right\} \cong \tan^{-1} \left\{ \tan(\pi\delta + \phi) - 2p \frac{\tilde{W}(2l+\delta)}{\tilde{W}(\delta)} \tan(\pi\delta + \phi) \right\}. \quad (\text{B.4})$$

By expressing the  $\tan^{-1}(\cdot)$  function using the Taylor's series about  $\tan(\pi\delta + \phi)$  truncated to the first order term, since  $\tilde{W}(\delta) \gg \tilde{W}(2l+\delta)$ , after some algebra (B.4) becomes:

$$\tan^{-1} \left\{ \tan(\pi\delta + \phi) - 2p \frac{\tilde{W}(2l+\delta)}{\tilde{W}(\delta)} \tan(\pi\delta + \phi) \right\} \cong \pi\delta + \phi + p \frac{\tilde{W}(2l+\delta)}{\tilde{W}(\delta)} \cos \left( 2\pi\delta + 2\phi + \frac{\pi}{2} \right). \quad (\text{B.5})$$

By replacing (B.5) into (B.2) it follows:

$$\text{angle}\{X_w(l)\} = -\frac{\pi}{2} + \pi\delta + \phi + p \frac{\tilde{W}(2l + \delta)}{\tilde{W}(\delta)} \cos\left(2\pi\delta + 2\phi + \frac{\pi}{2}\right), \quad (\text{B.6})$$

which substituted into (8) yields to:

$$\Delta\phi = -\pi\Delta\delta + p \frac{\tilde{W}(2l + \delta)}{\tilde{W}(\delta)} \cos\left(2\pi\delta + 2\phi + \frac{\pi}{2}\right). \quad (\text{B.7})$$

By expressing the error  $\Delta\delta$  using (A.7), from (B.7) the expression (10) is finally achieved.

## REFERENCES

1. D.C. Rife, G.A. Vincent, *Use of the discrete Fourier transform in the measurement of frequencies and levels of tones*, Bell System Technical Journal, **49**, pp. 197–228, 1970.
2. V.K. Jain, W.L. Collins, D.C. Davis, *High-accuracy analog measurements via interpolated FFT*, IEEE Transactions on Instrumentation and Measurement, **IM-28**, pp. 113–122, 1979.
3. T. Grandke, *Interpolation algorithms for discrete Fourier transforms of weighted signals*, IEEE Transactions on Instrumentation and Measurement, **IM-32**, 2, pp. 350–355, 1983.
4. C. Offelli, D. Petri, *The influence of windowing on the accuracy of multifrequency signal parameter estimation*, IEEE Transactions on Instrumentation and Measurement, **41**, 2, pp. 256–261, 1992.
5. D. Belega, D. Dallet, *Multifrequency signal analysis by interpolated DFT method with maximum sidelobe decay windows*, Measurement, **42**, 3, pp. 420–426, 2009.
6. D. Belega, D. Dallet, D. Petri, *Statistical description of the sine-wave frequency estimator provided by the interpolated DFT method*, Measurement, **45**, 1, pp. 109–117, 2012.
7. B.G. Quinn, *Estimation of frequency, amplitude, and phase from the DFT of a time series*, IEEE Transactions on Signal Processing, **45**, 3, pp. 814–817, 1997.
8. J. Schoukens, R. Pintelon, H. Van Hamme, *The interpolated fast Fourier transform: a comparative study*, IEEE Transactions on Instrumentation and Measurement, **41**, 2, pp. 226–232, 1992.
9. E. Aboutanios, B. Mulgrew, *Iterative frequency estimation by interpolation on Fourier coefficients*, IEEE Transactions on Signal Processing, **53**, 4, pp. 1237–1241, 2005.
10. Y. Liu, Z. Nie, Z. Zhao, Q.H. Liu, *Generalization of iterative Fourier interpolation algorithm for single frequency estimation*, Digital Signal Processing, **21**, 1, pp. 141–149, 2011.
11. D. Belega, D. Petri, *Frequency estimation by two- or three-point interpolated Fourier algorithms based on cosine windows*, Signal Processing, **114**, pp. 115–125, 2015.
12. F.J. Harris, *On the use of windows for harmonic analysis with the discrete Fourier transform*, Proceeding of IEEE, **66**, 1, pp. 51–83, 1978.
13. A.H. Nuttall, *Some windows with very good sidelobe behavior*, IEEE Transactions on Acoustic Speech and Signal Processing, **ASSP-29**, 1, pp. 84–91, 1981.
14. A. Ferrero, R. Ottoboni, *High-accuracy Fourier analysis based on synchronous sampling techniques*, IEEE Transactions on Instrumentation and Measurement, **41**, 6, pp. 780–785, 1992.
15. D. Belega, D. Dallet, D. Petri, *Modeling sine-wave image component contribution to discrete spectrum*, in: Proc. of the 19<sup>th</sup> IMEKO TC4 Symposium, July 18–19, 2013, Barcelona, Spain, pp. 722–726.

Received September 22, 2016